

First Flavor-Tagged Determination of Bounds on Mixing-Induced CP Violation in $B_s^0 \rightarrow J/\psi \phi$ Decays

The CDF Collaboration

The CDF author list to be inserted here.

(Dated: December 13, 2007)

Abstract

1 This Letter describes the first determination of bounds on the CP -violation parameter $2\beta_s$ using
2 B_s^0 decays in which the flavor of the bottom meson at production is identified. The result is based
3 on approximately 2,000 $B_s^0 \rightarrow J/\psi \phi$ decays reconstructed in a 1.35 fb^{-1} data sample collected with
4 the CDF II detector using $p\bar{p}$ collisions produced at the Fermilab Tevatron. We report confidence
5 regions in the two-dimensional space of $2\beta_s$ and the decay-width difference $\Delta\Gamma$. Assuming the
6 standard model predictions of $2\beta_s$ and $\Delta\Gamma$, the probability of a deviation as large as the level of
7 the observed data is 15%, corresponding to 1.5 Gaussian standard deviations.

8 Dedicated to the memory of our dear friend and colleague, Michael P. Schmidt.

PACS numbers: 13.25.Hw, 14.40.Nd, 14.65.Fy

9 The accurate determination of charge-conjugation-parity (CP) violation in meson sys-
10 tems has been one of the goals of particle physics since the effect was first discovered in
11 neutral kaon decays in 1964 [1]. Standard model CP -violating effects are described through
12 the Cabibbo-Kobayashi-Maskawa (CKM) mechanism [2], which has proved to be extremely
13 successful in describing the phenomenology of CP violation in B^0 and B^+ decays in the past
14 decade [3]. However, comparable experimental knowledge of B_s^0 decays has been lacking.

15 In the B_s^0 system, the mass eigenstates B_{sL}^0 and B_{sH}^0 are admixtures of the flavor eigen-
16 states B_s^0 and \bar{B}_s^0 . This causes oscillations between the B_s^0 and \bar{B}_s^0 states with a frequency
17 proportional to the mass difference of the mass eigenstates, $\Delta m_s \equiv m_H - m_L$. In the stan-
18 dard model this effect is explained in terms of second-order weak processes involving virtual
19 massive particles that provide a transition amplitude between the B_s^0 and \bar{B}_s^0 states. The
20 magnitude of this mixing amplitude is proportional to the oscillation frequency, while its
21 phase, responsible for CP violation in $B_s^0 \rightarrow J/\psi \phi$ decays, is $-2\beta_s^{SM} = -2 \arg \left(-\frac{V_{ts}V_{tb}^*}{V_{cs}V_{cb}^*} \right)$ [4],
22 where V_{ij} are the elements of the CKM quark mixing matrix. The presence of physics be-
23 yond the standard model could contribute additional processes and modify the magnitude
24 or the phase of the mixing amplitude. The recent precise determination of the oscillation
25 frequency [5] indicates that contributions of new physics to the magnitude, if any, are ex-
26 tremely small [6]. Global fits of experimental data tightly constrain the CP phase to small
27 values in the context of the standard model, $2\beta_s^{SM} \approx 0.04$ [7]. However, new physics may
28 contribute significantly larger values [6, 8]. The observed CP phase can be expressed as
29 $2\beta_s = 2\beta_s^{SM} - \phi_s^{NP}$, where ϕ_s^{NP} is due to the additional processes. The decay-width difference
30 between the mass eigenstates, $\Delta\Gamma \equiv \Gamma_L - \Gamma_H$, is also sensitive to the same new physics phase.
31 If $\phi_s^{NP} \gg 2\beta_s^{SM}$, we expect $\Delta\Gamma = 2|\Gamma_{12}| \cos(2\beta_s)$ [8], where $|\Gamma_{12}|$ is the off-diagonal element of
32 the B_s^0 - \bar{B}_s^0 decay matrix from the Schroedinger equation describing the time evolution of B_s^0
33 mesons [9]. Recent studies of $B_s^0 \rightarrow J/\psi \phi$ decays without identification of the initial flavor
34 of the B_s^0 meson [9, 10] have provided information on $\Delta\Gamma$ and have some limited sensitivity
35 to the CP phase.

36 In this Letter we present the first study of the $B_s^0 \rightarrow J/\psi \phi$ decay [11] in which the initial
37 state of the B_s^0 meson (*i.e.* whether it is produced as B_s^0 or its anti-particle \bar{B}_s^0) is identified
38 in a process known as “flavor tagging”. Such information is necessary to separate the time
39 evolution of mesons produced as B_s^0 or \bar{B}_s^0 . By relating this time development with the
40 CP eigenvalue of the final states, which is accessible through the angular distributions of the

41 J/ψ and ϕ mesons, we obtain direct sensitivity to the CP -violating phase. This phase enters
 42 the time-development with terms proportional to both $|\cos(2\beta_s)|$ and $\sin(2\beta_s)$. Analyses of
 43 $B_s^0 \rightarrow J/\psi \phi$ decays that do not use flavor tagging are primarily sensitive to $|\cos(2\beta_s)|$ and
 44 $|\sin(2\beta_s)|$, leading to a four-fold ambiguity in the determination of $2\beta_s$ [9, 10].

45 This measurement uses 1.35 fb^{-1} of data collected by the CDF experiment at the Fermilab
 46 Tevatron between February 2002 and September 2006. The CDF II detector is described in
 47 detail in Ref. [12]. Detector sub-systems relevant for this analysis are described briefly
 48 here. The tracking system is composed of silicon micro-strip detectors surrounded by a
 49 multi-wire drift chamber. The drift chamber provides tracking information and charged
 50 particle identification through the measurement of specific ionization energy loss (dE/dx).
 51 A time-of-flight (TOF) detector provides additional particle identification. These detectors
 52 are immersed within a 1.4 T axial magnetic field. Electromagnetic and hadronic calorimeters
 53 surround the solenoid. At the outermost radial extent of the detector, muons are detected
 54 in planes of multi-wire drift chambers and scintillators. The data used were collected with
 55 a di-muon trigger which preferentially selects events containing $J/\psi \rightarrow \mu^+ \mu^-$ decays [12].

56 We reconstruct the $B_s^0 \rightarrow J/\psi \phi$ decay from the decays $J/\psi \rightarrow \mu^+ \mu^-$ and $\phi \rightarrow K^+ K^-$
 57 and require these final state particles to originate from a common point. We use an artificial
 58 neural network (ANN) [13] to separate $B_s^0 \rightarrow J/\psi \phi$ signal from background. In the ANN
 59 training, we consider the following variables: particle identification of kaons using the TOF
 60 and dE/dx , the component of momenta of the B_s^0 and ϕ candidates transverse to the proton
 61 beam direction, the invariant mass of the ϕ candidate, and the quality of a kinematic fit to the
 62 trajectories of the final state particles. We have trained the ANN with signal events from sim-
 63 ulated data that are passed through the standard GEANT-based [14] simulation of the CDF II
 64 detector [15] and are reconstructed as in real data. We use $B_s^0 \rightarrow J/\psi \phi$ mass sideband can-
 65 didates, defined as those having $m(J/\psi \phi) \in [5.1820, 5.2142] \cup [5.3430, 5.3752] \text{ GeV}/c^2$, as
 66 the background sample in the ANN training. Applying the selection on the output variable
 67 of the ANN, we observe $2,019 \pm 73 B_s^0 \rightarrow J/\psi \phi$ signal events with a signal to background
 68 ratio of approximately one. The invariant $J/\psi \phi$ mass distribution is shown in Fig. 1. An
 69 event-specific primary interaction point is used in the calculation of the proper decay time,
 70 $t = m(B_s^0) L_{xy}(B_s^0) / p_T(B_s^0)$, where $L_{xy}(B_s^0)$ is the distance from the primary vertex to the
 71 $B_s^0 \rightarrow J/\psi \phi$ decay vertex projected onto the momentum of the B_s^0 in the plane transverse
 72 to the proton beam direction, $m(B_s^0)$ is the mass of the B_s^0 meson [3], and $p_T(B_s^0)$ is its

measured transverse momentum.

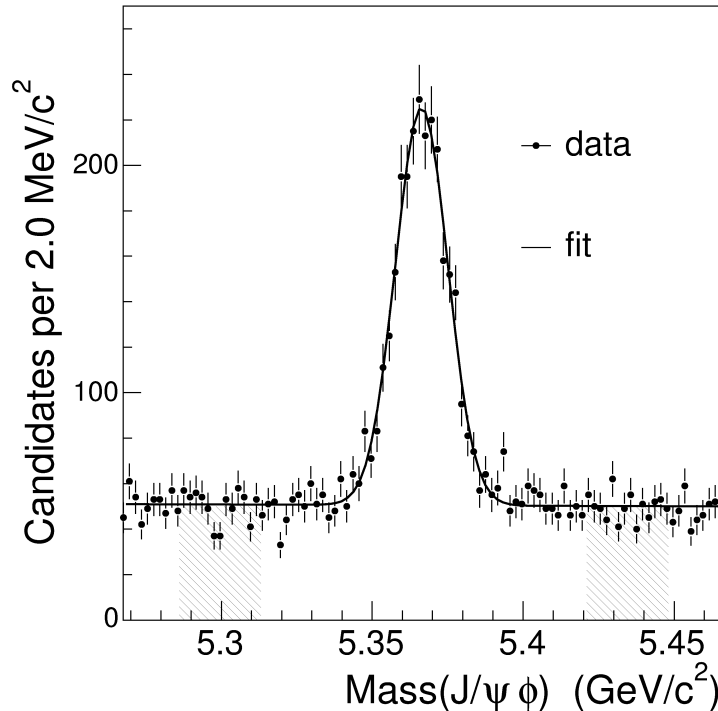


FIG. 1: Invariant $\mu^+\mu^-K^+K^-$ mass distribution with the fit projection overlaid. The hatched area indicates the mass sideband regions.

73

74 The orbital angular momenta of the vector (spin 1) mesons, J/ψ and ϕ , produced in the
 75 decay of the pseudoscalar (spin 0) B_s^0 meson, are used to distinguish the CP -even S- and D-
 76 wave final states from the CP -odd P-wave final state. We measure the decay angles θ_T , ϕ_T ,
 77 and ψ_T , defined in Ref. [9], in the transversity basis [16]. The transverse linear polarization
 78 amplitudes at $t = 0$, A_{\parallel} and A_{\perp} , correspond to CP even and CP odd final states, respectively.
 79 The longitudinal polarization amplitude A_0 corresponds to a CP even final state. The
 80 polarization amplitudes are required to satisfy the condition $|A_0|^2 + |A_{\parallel}|^2 + |A_{\perp}|^2 = 1$.

81 In order to separate the time development of the B_s^0 meson from that of the \bar{B}_s^0 meson,
 82 we identify the flavor of the B_s^0 or \bar{B}_s^0 meson at the time of production by means of flavor
 83 tagging. Two independent types of flavor tags are used, each exploiting specific features of
 84 the production of b quarks at the Tevatron, where they are mostly produced as $b\bar{b}$ pairs. The
 85 first type of flavor tag infers the production flavor of the B_s^0 or \bar{B}_s^0 meson from the decay
 86 products of the b hadron produced by the other b quark in the event. This is known as

87 an opposite-side flavor tag (OST). The OST decisions are based on the charge of muons or
 88 electrons from semileptonic B decays [17, 18] or the net charge of the opposite-side jet [19].
 89 If multiple tags are available for an event, the decision from the highest dilution flavor tag
 90 is chosen [20]. The tag dilution \mathcal{D} , defined by the probability to correctly tag a candidate
 91 $P_{tag} \equiv (1 + \mathcal{D})/2$, is estimated for each event. The calibration of the OST dilution is
 92 determined from $B^+ \rightarrow J/\psi K^+$ and $B^0 \rightarrow J/\psi K^{*0}$ decays. The second type of flavor tag
 93 identifies the flavor of the reconstructed B_s^0 or \bar{B}_s^0 meson at production by correlating it with
 94 the charge of an associated kaon arising from fragmentation processes [21], referred to as a
 95 same-side kaon tag (SSKT). The SSKT algorithm and its dilution calibration on simulated
 96 data are described in Ref. [22]. The average dilution is $(11 \pm 2)\%$ for the OST and $(27 \pm 4)\%$
 97 for the SSKT, where the uncertainties contain both statistical and systematic effects. The
 98 measured efficiencies for a candidate to be tagged are $(96 \pm 1)\%$ for the OST and $(50 \pm 1)\%$
 99 for the SSKT.

100 An unbinned maximum likelihood fit is performed to extract the parameters of interest,
 101 $2\beta_s$ and $\Delta\Gamma$, plus nuisance parameters to the measurement, which include the signal fraction
 102 f_s , the mean B_s^0 width $\Gamma \equiv (\Gamma_L + \Gamma_H)/2$, the mixing frequency Δm_s , the magnitudes of
 103 the polarization amplitudes $|A_0|^2$, $|A_{\parallel}|^2$, and $|A_{\perp}|^2$, and the strong phases $\delta_{\parallel} \equiv \arg(A_{\parallel}^* A_0)$
 104 and $\delta_{\perp} \equiv \arg(A_{\perp}^* A_0)$. The fit uses information on the reconstructed B_s^0 candidate mass m
 105 and its uncertainty σ_m , the B_s^0 candidate proper decay time t and its uncertainty σ_t , the
 106 transversity angles $\vec{\rho} = \{\cos\theta_T, \phi_T, \cos\psi_T\}$, and tag information \mathcal{D} and ξ , where \mathcal{D} is the
 107 event-specific dilution and $\xi = \{-1, 0, +1\}$ is the tag decision, in which $+1$ corresponds to
 108 a candidate tagged as B_s^0 , -1 to a \bar{B}_s^0 , and 0 to an untagged candidate. The single-event
 109 likelihood is described in terms of signal (P_s) and background (P_b) probability distribution
 110 functions (PDFs) as

$$\begin{aligned}
 & f_s P_s(m|\sigma_m) P_s(t, \vec{\rho}, \xi | \mathcal{D}, \sigma_t) P_s(\sigma_t) P_s(\mathcal{D}) \\
 & + (1 - f_s) P_b(m) P_b(t|\sigma_t) P_b(\vec{\rho}) P_b(\sigma_t) P_b(\mathcal{D}).
 \end{aligned} \tag{1}$$

111 The signal mass PDF $P_s(m|\sigma_m)$ is parameterized as a single Gaussian with a standard
 112 deviation determined separately for each candidate, while the background mass PDF, $P_b(m)$,
 113 is parameterized as a first order polynomial. The distributions of the decay time uncertainty
 114 and the event-specific dilution are observed to be different in signal and background, so we
 115 include their PDFs explicitly in the likelihood. The signal PDFs $P_s(\sigma_t)$ and $P_s(\mathcal{D})$ are

116 determined from sideband-subtracted data distributions, while the background PDFs $P_b(\sigma_t)$
 117 and $P_b(\mathcal{D})$ are determined from the $J/\psi\phi$ invariant mass sidebands. The PDFs of the
 118 decay time uncertainties, $P_s(\sigma_t)$ and $P_b(\sigma_t)$, are described with a sum of Gamma function
 119 distributions, while the dilution PDFs $P_s(\mathcal{D})$ and $P_b(\mathcal{D})$ are included as histograms that
 120 have been extracted from data.

121 The time and angular dependence of the signal PDF $P_s(t, \vec{\rho}, \xi, |\mathcal{D}, \sigma_t)$ for a single flavor
 122 tag can be written in terms of two PDFs, P for B_s^0 and \bar{P} for \bar{B}_s^0 , as

$$P_s(t, \vec{\rho}, \xi | \mathcal{D}, \sigma_t) = \frac{1 + \xi \mathcal{D}}{2} P(t, \vec{\rho} | \sigma_t) \epsilon(\vec{\rho}) + \frac{1 - \xi \mathcal{D}}{2} \bar{P}(t, \vec{\rho} | \sigma_t) \epsilon(\vec{\rho}), \quad (2)$$

123 which is trivially extended in the case of two independent flavor tags (OST and SSKT).
 124 The detector acceptance effects on the transversity angle distributions, $\epsilon(\vec{\rho})$, are modeled
 125 with $B_s^0 \rightarrow J/\psi\phi$ simulated data. Three-dimensional joint distributions of the transversity
 126 angles are used to determine $\epsilon(\vec{\rho})$, in order to correctly account for any dependencies among
 127 the angles. The time and angular probabilities for B_s^0 can be expressed as

$$\begin{aligned} \frac{d^4 P(t, \vec{\rho})}{dt d\vec{\rho}} &\propto |A_0|^2 \mathcal{T}_+ f_1(\vec{\rho}) + |A_{\parallel}|^2 \mathcal{T}_+ f_2(\vec{\rho}) \\ &+ |A_{\perp}|^2 \mathcal{T}_- f_3(\vec{\rho}) + |A_{\parallel}| |A_{\perp}| \mathcal{U}_+ f_4(\vec{\rho}) \\ &+ |A_0| |A_{\parallel}| \cos(\delta_{\parallel}) \mathcal{T}_+ f_5(\vec{\rho}) \\ &+ |A_0| |A_{\perp}| \mathcal{V}_+ f_6(\vec{\rho}), \end{aligned} \quad (3)$$

128 where the functions $f_1(\vec{\rho}) \dots f_6(\vec{\rho})$ are defined in Ref. [9]. The probability \bar{P} for \bar{B}_s^0 is
 129 obtained by substituting $\mathcal{U}_+ \rightarrow \mathcal{U}_-$ and $\mathcal{V}_+ \rightarrow \mathcal{V}_-$. The time-dependent term \mathcal{T}_{\pm} is defined
 130 as

$$\begin{aligned} \mathcal{T}_{\pm} = e^{-\Gamma t} &\times [\cosh(\Delta\Gamma t/2) \mp \cos(2\beta_s) \sinh(\Delta\Gamma t/2) \\ &\mp \eta \sin(2\beta_s) \sin(\Delta m_s t)], \end{aligned}$$

131 where $\eta = +1$ for P and -1 for \bar{P} . The other time-dependent terms are defined as

$$\begin{aligned}
\mathcal{U}_{\pm} &= \pm e^{-\Gamma t} \times [\sin(\delta_{\perp} - \delta_{\parallel}) \cos(\Delta m_s t) \\
&\quad - \cos(\delta_{\perp} - \delta_{\parallel}) \cos(2\beta_s) \sin(\Delta m_s t) \\
&\quad \pm \cos(\delta_{\perp} - \delta_{\parallel}) \sin(2\beta_s) \sinh(\Delta\Gamma t/2)], \\
\mathcal{V}_{\pm} &= \pm e^{-\Gamma t} \times [\sin(\delta_{\perp}) \cos(\Delta m_s t) \\
&\quad - \cos(\delta_{\perp}) \cos(2\beta_s) \sin(\Delta m_s t) \\
&\quad \pm \cos(\delta_{\perp}) \sin(2\beta_s) \sinh(\Delta\Gamma t/2)].
\end{aligned}$$

132 These relations assume that there is no direct CP violation in the system. The time-
133 dependence is convolved with a Gaussian proper time resolution function with standard
134 deviation σ_t , which is adjusted by an overall calibration factor determined from the fit using
135 promptly decaying background candidates. The average of the resolution function is 0.1 ps,
136 with a root-mean-square deviation of 0.04 ps.

137 We model the lifetime PDF for the background, $P_b(t|\sigma_t)$, with a delta function at $t = 0$,
138 a single negative exponential, and two positive exponentials, all of which are convolved with
139 the Gaussian resolution function. The background angular PDFs are factorized, $P_b(\vec{\rho}) =$
140 $P_b(\cos\theta_T)P_b(\varphi_T)P_b(\cos\psi_T)$, and are obtained using B_s^0 mass sidebands events.

141 Possible asymmetries between the tagging rate and dilution of B_s^0 and \bar{B}_s^0 mesons have
142 been studied with control samples and found to be statistically insignificant. We allow
143 important sources of systematic uncertainty, such as the determination of overall calibration
144 factors associated with the proper decay time resolution and the dilutions, to float in the
145 fit. The mixing frequency $\Delta m_s = 17.77 \pm 0.12 \text{ ps}^{-1}$ is constrained in the fit within the
146 experimental uncertainties [5]. Systematic uncertainties coming from alignment, detector
147 sculpting, background angular distributions, decays from other B mesons, the modeling of
148 signal and background are found to have a negligible effect on the determination of both
149 $\Delta\Gamma$ and β_s relative to statistical uncertainties.

150 An exact symmetry is present in the signal probability distribution, as can be seen
151 in Eq. (3), which is invariant under the simultaneous transformation ($2\beta_s \rightarrow \pi - 2\beta_s$,
152 $\Delta\Gamma \rightarrow -\Delta\Gamma$, $\delta_{\parallel} \rightarrow 2\pi - \delta_{\parallel}$, and $\delta_{\perp} \rightarrow \pi - \delta_{\perp}$). This causes the likelihood function to have two
153 minima. This symmetry can be removed by restricting any of the above parameters within
154 appropriate ranges. However, even after removal of the exact symmetry, approximate sym-
155 metries remain, producing local minima. Since the log-likelihood function is non-parabolic,

156 we cannot meaningfully quote point estimates. Instead we choose to construct a confidence
 157 region in the $2\beta_s - \Delta\Gamma$ plane.

158 We use the Feldman-Cousins likelihood ratio ordering [23] to determine the confidence
 159 level (CL) for a 20×40 grid evenly spaced in $2\beta_s \in [-\pi/2, 3\pi/2]$ and $\Delta\Gamma \in [-0.7, 0.7]$.
 160 The other parameters in the fit are treated as nuisance parameters (*e.g.* B_s^0 mean width,
 161 transversity amplitudes, strong phases) [24]. The coverage against deviations of the nuisance
 162 parameters from the measured values is confirmed by randomly sampling the nuisance pa-
 163 rameter space within $\pm 5\sigma$ of the values determined from the fit to data. The 68% and 95%
 164 confidence regions obtained are shown in Fig. 2. The solution centered in $0 \leq 2\beta_s \leq \pi/2$
 165 and $\Delta\Gamma > 0$ corresponds to $\cos(\delta_\perp) < 0$ and $\cos(\delta_\perp - \delta_\parallel) > 0$, while the opposite is true
 166 for the solution centered in $\pi/2 \leq \beta_s \leq \pi$ and $\Delta\Gamma < 0$. Assuming the standard model pre-
 167 dicted values of $2\beta_s = 0.04$ and $\Delta\Gamma = 0.096 \text{ ps}^{-1}$ [8], the probability to observe a likelihood
 168 ratio equal to or higher than what is observed in data is 15%. Additionally, we present a
 169 Feldman-Cousins confidence interval of $2\beta_s$, where $\Delta\Gamma$ is treated as a nuisance parameter,
 170 and find that $2\beta_s \in [0.32, 2.82]$ at the 68% confidence level. The CP phase $2\beta_s$, $\Delta\Gamma$, Γ , and
 171 the linear polarization amplitudes are consistent with those measured in Ref. [9].

172 We also exploit current experimental and theoretical information to extract tighter
 173 bounds on the CP -violating phase. By applying the constraint $|\Gamma_{12}| = 0.048 \pm 0.018$ [8] in
 174 the relation $\Delta\Gamma = 2|\Gamma_{12}| \cos(2\beta_s)$, we obtain $2\beta_s \in [0.24, 1.36] \cup [1.78, 2.90]$ at the 68% CL . If
 175 we additionally constrain the strong phases δ_\parallel and δ_\perp to the results from $B^0 \rightarrow J/\psi K^{*0}$ de-
 176 cays [25] and the B_s^0 mean width to the world average B^0 width [3], we find $2\beta_s \in [0.40, 1.20]$
 177 at the 68% CL .

178 In summary we present confidence bounds on the CP -violation parameter $2\beta_s$ and the
 179 width difference $\Delta\Gamma$ from the first measurement of $B_s^0 \rightarrow J/\psi \phi$ decays using flavor tagging.
 180 Assuming the standard model predicted values of $2\beta_s = 0.04$ and $\Delta\Gamma = 0.096 \text{ ps}^{-1}$, the
 181 probability of a deviation as large as the level of the observed data is 15%, which corresponds
 182 to 1.5 Gaussian standard deviations. Treating $\Delta\Gamma$ instead as a nuisance parameter and fitting
 183 only for $2\beta_s$, we find that $2\beta_s \in [0.32, 2.82]$ at the 68% confidence level. The presented
 184 experimental bounds restrict the knowledge of $2\beta_s$ to two of the four solutions allowed in
 185 measurements that do not use flavor tagging [9, 10] and improve the overall knowledge of
 186 this parameter.

187 We would like to thank U. Nierste for several useful suggestions. We thank the Fermilab

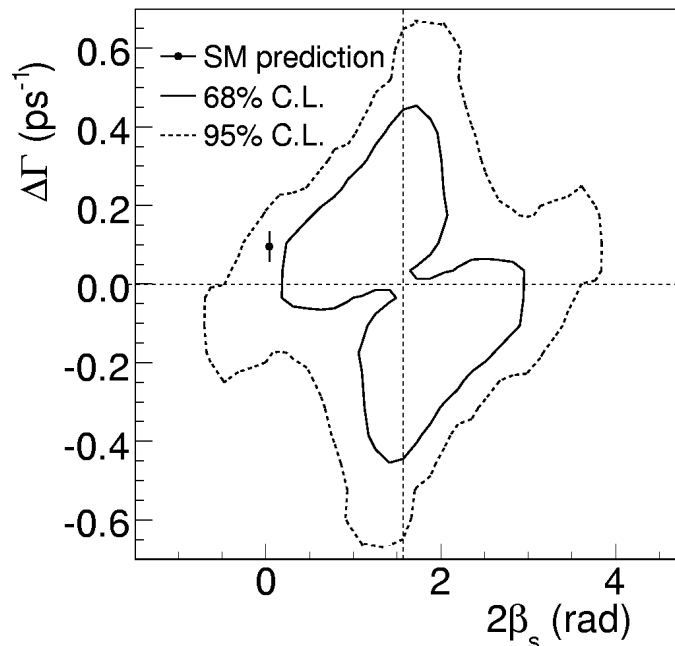


FIG. 2: Feldman-Cousins confidence region in the $2\beta_s - \Delta\Gamma$ plane, where the standard model favored point is shown with error bars [8]. The intersection of the horizontal and vertical dotted lines indicates the reflection symmetry in the $2\beta_s - \Delta\Gamma$ plane.

188 staff and the technical staffs of the participating institutions for their vital contributions.
 189 This work was supported by the U.S. Department of Energy and National Science Founda-
 190 tion; the Italian Istituto Nazionale di Fisica Nucleare; the Ministry of Education, Culture,
 191 Sports, Science and Technology of Japan; the Natural Sciences and Engineering Research
 192 Council of Canada; the National Science Council of the Republic of China; the Swiss Na-
 193 tional Science Foundation; the A.P. Sloan Foundation; the Bundesministerium für Bildung
 194 und Forschung, Germany; the Korean Science and Engineering Foundation and the Korean
 195 Research Foundation; the Science and Technology Facilities Council and the Royal Society,
 196 UK; the Institut National de Physique Nucleaire et Physique des Particules/CNRS, France;
 197 the Russian Foundation for Basic Research; the Comisión Interministerial de Ciencia y Tec-
 198 nología, Spain; the European Community's Human Potential Programme; the Slovak R&D
 199 Agency; and the Academy of Finland.

-
- 200 [1] J. H. Christenson et al., Phys. Rev. Lett. **13**, 138 (1964).
- 201 [2] N. Cabibbo, Phys. Rev. Lett. **10**, 531 (1963),
- 202 M. Kobayashi and T. Maskawa, Prog. Theor. Phys. **49**, 652 (1973).
- 203 [3] W.-M. Yao et al. (Particle Data Group), J. Phys. G **33**, 1 (2006).
- 204 [4] I. Dunietz, R. Fleischer, and U. Nierste, Phys. Rev. D **63**, 114015 (2001).
- 205 [5] A. Abulencia et al. (CDF Collaboration), Phys. Rev. Lett. **97**, 242003 (2006).
- 206 [6] Z. Ligeti, M. Papucci, and G. Perez, Phys. Rev. Lett **97**, 101801 (2006).
- 207 [7] E. Barberio et al. (Heavy Flavor Averaging Group) (2007), arXiv:hep-ex/0603003.
- 208 [8] A. Lenz and U. Nierste, J. High Energy Phys. **06**, 072 (2007).
- 209 [9] ArXiv:hep-ex/.... (CDF note 9100), to be submitted to PRL.
- 210 [10] V. M. Abazov et al. (D0 Collaboration), Phys. Rev. Lett. **98**, 121801 (2007).
- 211 [11] Charge-conjugate states are implied throughout the paper unless otherwise specified.
- 212 [12] D. Acosta et al. (CDF Collaboration), Phys. Rev. D **71**, 032001 (2005).
- 213 [13] A. Zell et al., *SNNS, Stuttgart Neural Network Simulator, User manual, Version 3.2* (Univer-
- 214 sity of Stuttgart, Comp. Science Dept., Report No. 6/94, 1994).
- 215 [14] R. Brun et al., CERN-DD-78-2-REV (1978).
- 216 [15] E. Gerchtein and M. Paulini, ECONF **C0303241**, TUMT005 (2003), arXiv:physics/0306031.
- 217 [16] A. S. Dighe, I. Dunietz, and R. Fleischer, Eur. Phys. J. C **6**, 647 (1999).
- 218 [17] G. Giurgiu, Ph.D. thesis, Carnegie Mellon Univ., FERMILAB-THESIS-2005-41 (2005).
- 219 [18] V. Tiwari, Ph.D. thesis, Carnegie Mellon Univ., FERMILAB-THESIS-2007-09 (2007).
- 220 [19] C. Lecci, Ph.D. thesis, Univ. of Karlsruhe, FERMILAB-THESIS-2005-89 (2005).
- 221 [20] A. Abulencia et al. (CDF Collaboration), Phys. Rev. Lett. **97**, 062003 (2006).
- 222 [21] A. Ali and F. Barreiro, Z. Phys. C **30**, 635 (1986),
- 223 M. Gronau, A. Nippe, J. L. Rosner, Phys. Rev. D **47**, 1988 (1993), M. Gronau and J. L. Rosner,
- 224 Phys. Rev. D **49**, 254 (1994).
- 225 [22] A. Belloni, Ph.D. thesis, MIT, FERMILAB-THESIS-2007-36 (2007).
- 226 [23] G. J. Feldman and R. D. Cousins, Phys. Rev. **D57**, 3873 (1998).
- 227 [24] A. C. Davison and D. V. Hinkley, *Bootstrap methods and their applications* (Cambridge Uni-
- 228 versity Press, 1997).

229 [25] B. Aubert et al. (*BABAR* Collaboration), Phys. Rev. D **71**, 032005 (2005).